

# Investigation of Nb/VGd/Nb/Al<sub>2</sub>O<sub>3</sub> Multilayered Structure by Polarized Neutron Reflectometry

## Abstract

The Nb(15 nm)/V(70 nm)/Gd(3 nm)/Nb(100 nm)/Al<sub>2</sub>O<sub>3</sub> layered structure has been investigated using polarized neutron reflectometry at temperature  $T = 1.5$  K and  $T = 12$  K in magnetic field equals to 500 Oe. Reflectivities of both spin-up and spin-down were measured showing three peaks when plotted against the neutron wavelength. Neutron spin asymmetry of both measurements demonstrate that the behavior of both curves has not been changed in this temperature limit.

## Introduction

Several studies were done on the phenomenon of coexistence of superconductivity and ferromagnetism in layered structure [1]. Superconductor/ferromagnet structures exhibit the proximity effect, which is represented in the penetration of superconducting pairs from the superconducting layer into the ferromagnetic layer and establishment of a superconducting order parameter and a ferromagnetic order parameter modified by superconductivity in the ferromagnetic layer. Along with the proximity effect, the reverse proximity effect may occur in superconductor/ferromagnet structures [2, 3], which implies magnetization of the superconducting layer. Due to the diverse set of inverse proximity effect, including the Fulde-Ferrel-Larkin-Ovchinnikov phase,  $\pi$ -phase superconductivity, and triplet pairing, the superconducting (S) and ferromagnetic (F) layers are attracting great attention. On the other hand, the proximity effect where superconductivity influences ferromagnetism have received less attention. Triplet superconductivity may exist in noncollinear superconductor/ferromagnet structures [4]. A triplet pair, having nonzero spin, can penetrate deeper into the ferromagnetic layer in comparison with a Cooper pair.

For most S/F heterostructures composed of elemental metals or alloys,  $T_f$  greatly exceeds  $T_c$ . In such case one still expects significant magnetic proximity effects if the effective energy  $E_f \sim T_f d_f/d_s$  becomes comparable to  $E_s \sim T_c$ , where  $d_f$  ( $d_s$ ) are the thicknesses of the F(S) layers. The first to indicate such a possibility were Anderson and Suhl. They considered systems consisting of S and F phases and come

to the conclusion that a homogeneous magnetic phase above  $T_c$  may become inhomogeneous below  $T_c$ . Such a transition, which they called cryptoferromagnetism (CFM), would depress the effective exchange field of ferromagnetism, thus enabling the coexistence of superconductivity and magnetism. Penetration of the magnetic order also occurs on a length scale of  $\xi$ , which for conventional superconductors is typically 10-100 nm. This is a long-range effect caused by exchange interaction. The sign of the induced magnetization depends on the quality of the S/F interface. In [2] and [5], the transport through the S/F interface was considered in the diffusive limit, i.e., for the case of highly disordered (rough, dirty) interfaces. The induced magnetization of the diffusive limit points antiparallel to the magnetization of the FM layer [6]. On the contrary, for a smooth (clean) S/F interface the ballistic limit applies and a parallel orientation of the FM and the induced magnetization is expected [6]. Therefore, the quality of the S/F interface plays an important role in the considered problem. The temperature dependence of the magnetic proximity effect is investigated in many articles [2, 7, 8]. In all cases, the proximity effect is manifested and most pronounced at temperatures far below  $T_c$ , the superconducting transition temperature. Upon rising the temperature to  $T_c$ , the induced magnetization gradually vanishes.

A potential candidate for S/F systems is a Gd/Nb heterostructure. One of the advantages of gadolinium is that it is a weak ferromagnet with Curie temperature  $T_f = 293$  K which in combination with Nb, the strongest elemental superconductor with bulk  $T_c = 9.3$  K, allows for preparation of S/F systems with comparable ferromagnetic and superconducting energies. Moreover, gadolinium is able to couple with other ferromagnets [9, 10] forming non-trivial magnetic ordering patterns which can be used for the creation of superconducting spin valves. In [11], Nb(25nm)/Gd( $d_f$ )/Nb(25nm) trilayers have been studied showing that the structures with highly transparent S/F interfaces and rather high correlation length can be grown.

Experimental observation of the magnetic proximity effect requires methods which on one hand are of high sensitivity, and on the other hand, provide a measure of the distribution of the magnetic moment within the S/F heterostructures with a resolution much less than  $\xi$ , one such method, as we will see in the next section, is polarized neutron reflectometry (PNR). This method has already been used to study the magnetic state of S/F systems.

In the present work, we report on Nb(15 nm)/V(70 nm)/Gd(3 nm)/Nb(100 nm)/Al<sub>2</sub>O<sub>3</sub> multilayers using PNR for investigations. In the PNR experiment, spin-up  $R^{++}$  and spin-down  $R^{-}$  reflectivities were measured as a function of the neutron

wavelength. The neutron spin asymmetry  $S \equiv (R^{++} - R^{--})/(R^{++} + R^{--})$  was calculated and get compared with theoretical values of the neutron spin asymmetry.

The aim of the work is finding a good fitting for the experimental results of the mentioned structure.

## Polarized Neutron Reflectometry

The scheme of a typical PNR experiment is shown in Fig. 1. The neutron beam of wavelength  $\lambda$  is polarized by the polarizer P (a magnetic supermirror [12]) the transmission of which is dependent on the neutron spin direction. The polarized beam is then collimated by slits and directed to the sample (SM in fig. 1) at an angle of incidence  $\theta_1$ . The neutron beam is scattered at an exit angle  $\theta_2$ . The polarization of the scattered beam is analyzed by the analyzer of polarization AP, the operating principle of which is the same as of P. The intensity transmitted through AP is recorded by the detector D. The beam polarization direction to the guide magnetic field in front of and behind the sample is periodically reversed by the spin-flippers  $SF_1$  and  $SF_2$ .

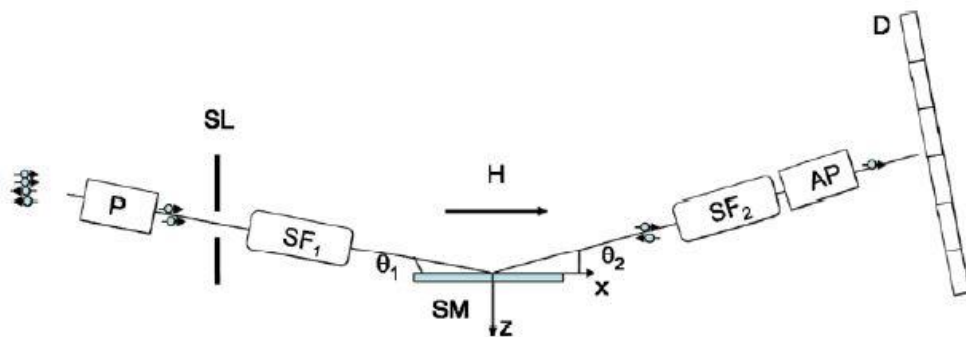


Figure 1 PNR experimental scheme. P — polarizer, SL — slit,  $SF_{1(2)}$  — spin flippers, H — external magnetic field, SM — sample, AP — analyzer of the polarization, D — detector.

The measured quantities in PNR experiments are intensities of the specular reflection ( $\theta_1 = \theta_2$ ) and of the diffuse scattering ( $\theta_1 \neq \theta_2$ ) at different angles of incidence and states of the spin flippers (on – on, off – off, on – off, off – on). The

primary data treatment procedure consists of taking into account the background intensity as well as  $P_p$ ,  $P_a$ ,  $P_{SF1}$ , and  $P_{SF2}$  the efficiencies of the polarizer, the analyzer and the spin flippers, respectively. As a result of this data processing, one obtains the reflectivities  $R^{\mu\nu}(Q)$  as a function of momentum transfer  $Q$ , normalized to the intensity of the incident beam. Here, the indices  $\mu$  and  $\nu$  take the values “+” or “-” and correspond to the projection of the neutron spin on the guide field before and after the scattering process, respectively. Experimental reflectivities are then compared with theoretical values. The latter are calculated varying the optical potential of the neutrons in the investigated system.

In the most general case, the optical potential is a function of the three space coordinates and has nuclear and magnetic contributions:

$$V = 4 \pi \rho_N + c \sigma \mathbf{B}, \quad (1)$$

where  $\rho_N$  is the nuclear scattering length density (SLD), which depends on the nuclear density and the coherent scattering length of each nucleus which is different for different atoms and isotopes [13]. The magnetic component is proportional to the scalar product of the Pauli matrix vector  $\sigma$  and the vector of magnetic induction in the medium  $\mathbf{B}$ . The scaling factor is  $c = (-2m/\hbar^2)\mu_n$ , where  $m$  and  $\mu_n$  are the mass and the magnetic moment of the neutron, respectively, and  $\hbar$  is the Planck constant. For a stratified medium, the optical potential depends on a single space coordinate, the one perpendicular to the layers. For this special case, the solution of the Schrödinger equation can be obtained analytically [14–16]. Here, we will present simple approximations to demonstrate the dependence of the reflectivity on the components of the optical potential in the different scattering channels. In particular, the amplitude of non-spin-flip specular scattering in the Born approximation can be written as

$$r^{--(++)}(Q) \approx \frac{1}{Q_z^2} \int \frac{\partial}{\partial z} [4 \pi \rho_N(z) \pm c B_{||}(z)] e^{iQ_z z} dz, \quad (2)$$

where  $Q_z = 4\pi \sin\theta_1/\lambda$  is the momentum transfer component perpendicular to the sample surface, and where)  $B_{||}(z) = B(z) \cos\alpha(z)$  is the depth-profile of the component of the magnetic induction parallel to the neutron beam polarization vector ( $\alpha$  is the angle between  $\mathbf{B}$  and the polarization vector). From expression (2), it can be seen that the amplitude  $r^{++}(r^{--})$  is a sum (difference) of Fourier transforms of the derivatives of the nuclear profile and  $B_{||}(z)$ :

$$r^{--(++)} = r_0 \pm r_{||}^{mag}, \quad (3)$$

where  $r_0$  and  $r_{||}^{mag}$  are the reflection amplitudes due to a pure nuclear profile and  $B_{||}(z)$ , respectively. For a weak magnetic system ( $|cB| \ll |4\pi\rho|$ ), one has  $r_0 \gg r_{||}^{mag}$ , so that, the reflectivities  $R^{--(++)} \equiv |r^{--(++)}|^2$  are primarily sensitive to the nuclear profile. In order to separate the magnetic contribution in the reflectivity, it is convenient to use the so-called spin asymmetry  $S(Q) \equiv [R^{++} - R^{--}]/[R^{++} + R^{--}]$ .

## Experimental

The samples of the nominal structure Nb(15nm)/V(70nm)/Gd(3,6,12nm)/Nb(100nm) (here and later SFS<sub>x</sub>, where  $x \equiv d_f$  measured in nanometers) were prepared using an UHV magnetron machine ULVAC MPS-4000-C6 at constant current on Al<sub>2</sub>O<sub>3</sub>(1 $\bar{1}$ 02) substrates (see Fig. 2). The bilayer Nb/V on the top is required to protect against oxidation and to create a neutron waveguide structure.

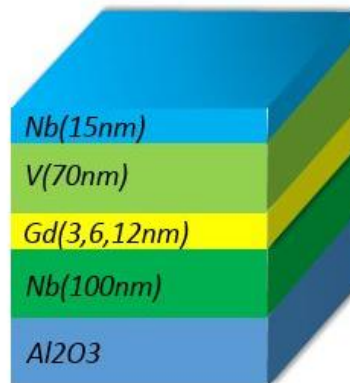


Figure 2 shows the general design of the prepared structure.

Polarized neutron reflectometry (PNR) was used as a depth-sensitive magnetometric method. The PNR experiments were conducted on REMUR at the research reactor IBR-2 (Dubna, Russia).

The sample was cooled from temperature  $T = 300$  K to  $T = 12$  K in magnetic field strength  $H = 20$  Oe. At  $T = 12$  K, the sample was magnetized at  $H = 1.9$  KOe for one minute. Then, the magnetic field strength was reduced to  $H = 500$  Oe and the spin-polarized neutron reflectivities were measured. The temperature of the sample was then decreased to  $T = 1.5$  K and measurements were taken again. Fig. 3 shows

the spin-up and spin-down neutron reflectivities of the sample at  $T = 12 \text{ K}$  and  $T = 1.5 \text{ K}$  in magnetic field strength equals to  $500 \text{ Oe}$ .

Fig. 3 shows the dependence of spin-up and spin-down reflectivities at temperatures equal  $1.5 \text{ K}$  and  $12 \text{ K}$  and magnetic field strength equals  $500 \text{ Oe}$ . For the calculations, the layers in the structure were divided into sublayer. It is obvious that the reflectivity of both spin-up  $R^{++}$  (red curve) and spin-down  $R^{--}$  (black curve) of the sample at  $T = 1.5 \text{ K}$  have almost the same behavior. Similarly, the reflectivity of both spin-up  $R^{++}$  (green curve) behaves exactly the same as spin-down  $R^{--}$  (blue curve) at  $T = 12 \text{ K}$ . Raising the temperature of the sample at the same field strength led to increasing the amplitude of the reflectivities of spin-up and spin-down as it is displayed in the figure. These curves exhibit three Bragg peaks.

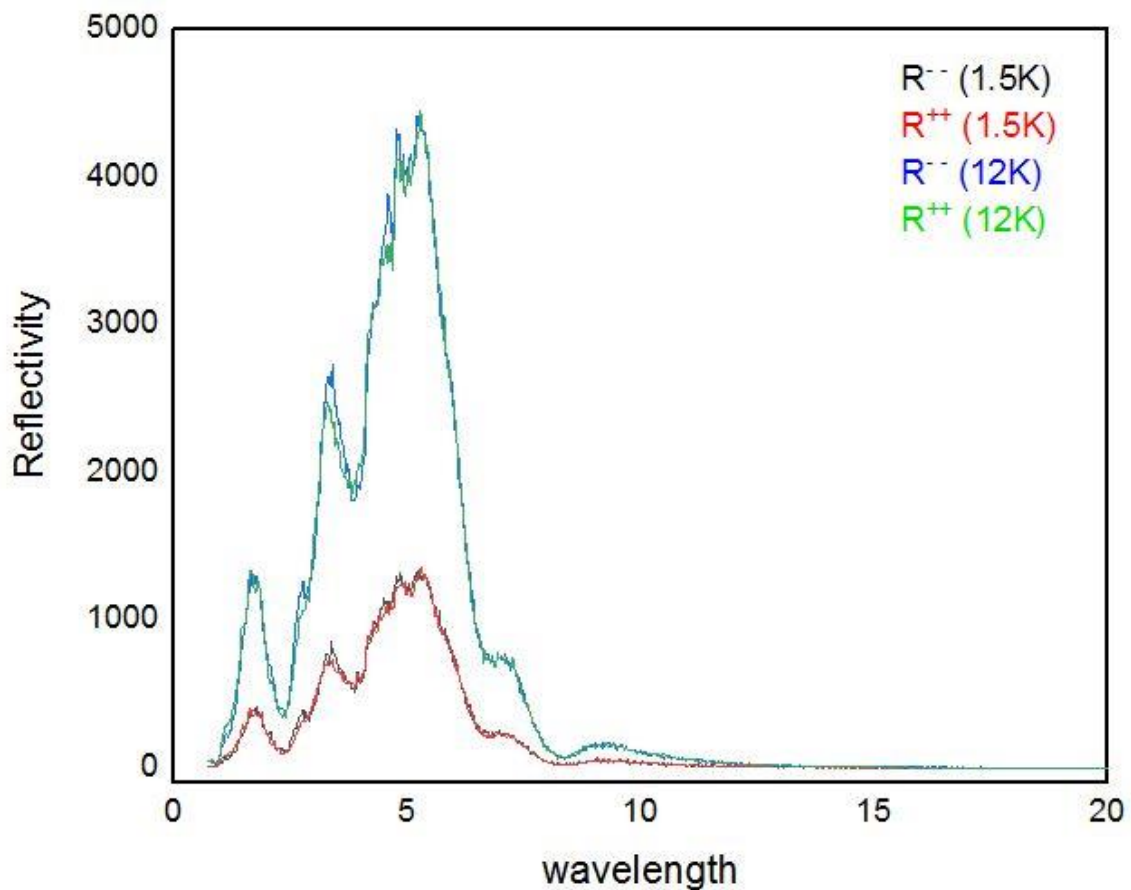


Figure 3 The dependence of Reflectivities on neutron wavelength at  $T = 1.5 \text{ K}$  and  $T = 12 \text{ K}$  and  $H = 500 \text{ Oe}$ .

The spin asymmetry at temperatures of 1.5 and 12 kelvins along with the calculated one are shown in fig. 4. The nonzero spin asymmetry evidences the presence of a magnetic moment in the system. The two curves appeared to have similar behavior.

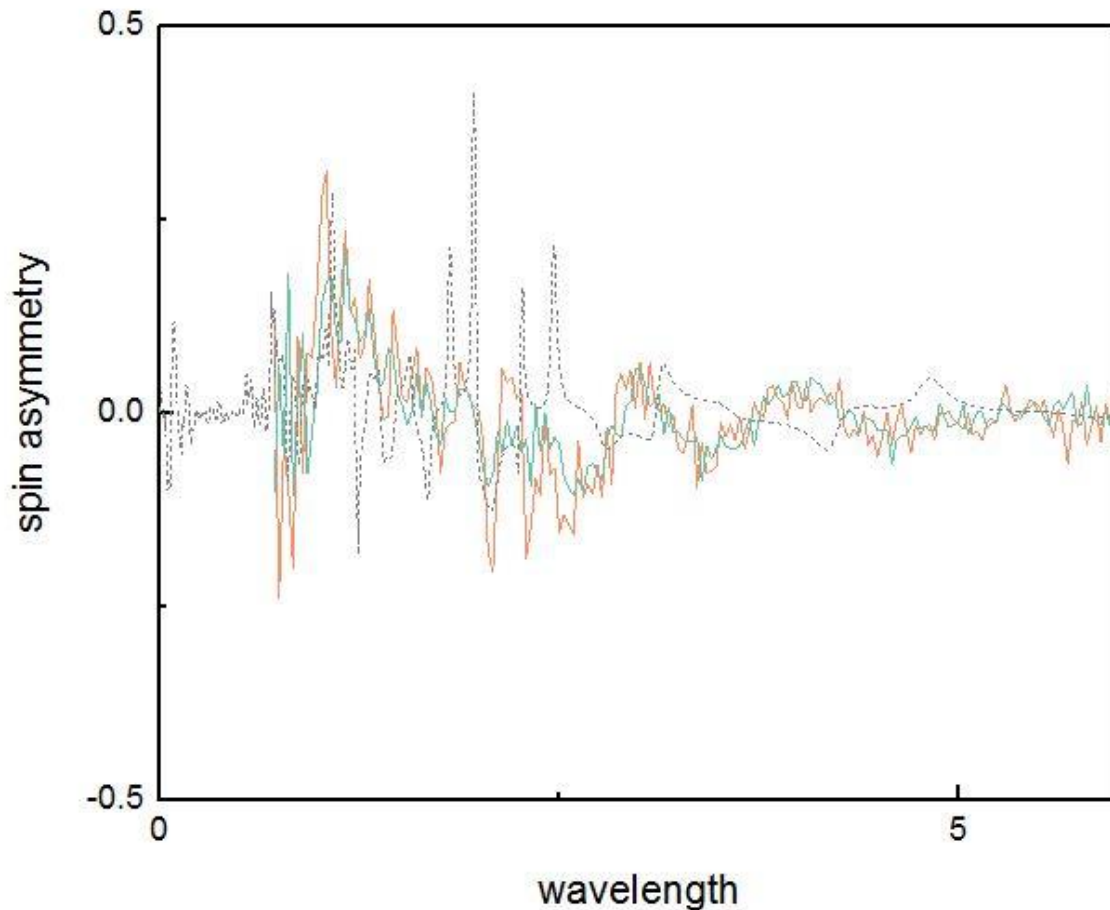


Figure 4 Spin asymmetries at  $T = 1.5$  K (orange solid line) and  $T = 12$  K (green solid line) and calculated (grey dashed line) at  $H = 500$  Oe.

## Conclusion and Discussion

As a result of the investigation of the Nb(15 nm)/V(70 nm)/Gd(3 nm)/Nb(100 nm)/Al<sub>2</sub>O<sub>3</sub> structure by polarized neutron reflectometry, the reflectivities of spin-up and spin-down were measured at different temperatures of 1.5 K and 12 K in the magnetic field strength 500 Oe. The reflectivities of both spins at the same temperature appear to have almost the same behavior. But with changing temperatures, the reflectivities are changed consequently. Spin asymmetries were also found experimentally and theoretically for different temperatures. There was not a great change in the spin asymmetries curves when the temperature changed.

## Acknowledgement

I would like to thank Prof. Vladimir Zhaketov for his assistance and his fruitful discussions.

## References

- [1] Yu. A. Izyumov, Yu. N. Proshin, and M. G. Khusainov, *Usp. Fiz. Nauk* 45 (2), 109 (2002).
- [2] F. S. Bergeret, A. F. Volkov, and K. B. Efetov, *Phys. Rev. B: Condens. Matter Mater. Phys.* 69, 174 504 (2004).
- [3] V. N. Krivoruchko and E. A. Koshina, *Phys. Rev. B: Condens. Matter Mater. Phys.* 66, 014 521 (2002).
- [4] A. F. Volkov, F. S. Bergeret, and K. B. Efetov, *Phys. Rev. Lett.* 90, 117 006 (2003).
- [5] Krivoruchko, V.N., Koshina, E.A.: *Phys. Rev. B* 66, 014521 (2002).
- [6] Bergeret, F.S., et al.: *Phys. Rev. B* 72, 064524 (2005).
- [7] Halterman, K., Valls, O.T.: *Phys. Rev. B* 69, 014517 (2004).
- [8] Lofwander, T., et al.: *Phys. Rev. Lett.* 95, 187003 (2005).
- [9] Drovosekov A B, Savitsky A O, Kholin D I, Kreines N M, Proglyado V V, Makarova M V, Kravtsov E A and Ustinov V V 2019, *J. Magn. Magn. Mater.* 475 668.
- [10] Antropov N O, Kravtsov E A, Khaidukov Yu N, Ryabukhina M V, Proglyado V V, Weschke O and Ustinov V V 2018 *JETP Lett.* 108 341.
- [11] Khaydukov Yu N et al 2018 *Phys. Rev. B* 97 144511.
- [12] Schebetov, A.F., et al.: *Nucl. Instrum. Methods B* 94, 575 (1994).
- [13] <http://www.ncnr.nist.gov/resources/sldcalc.html>
- [14] Pleshanov, N.K., Pusenkov, V.M.: *Z. Phys. B* 100, 507 (1996).
- [15] Radu, F., Ignatovich, V.K.: *Physica B* 267, 175 (1999).
- [16] Rühm, A., et al.: *Phys. Rev. B* 60, 16073 (1999).